VALIDATION OF CFD MODELLING OF LH$_2$ SPREAD AND EVAPORATION AGAINST LARGE-SCALE SPILL EXPERIMENTS

Prankul Middha[*]**, Mathieu Ichard, Bjørn J. Arntzen**
GexCon AS, P.O. Box 6015, NO-5892 Bergen, Norway

ABSTRACT

Hydrogen is widely recognized as an attractive energy carrier due to its low-level air pollution and its high mass-related energy density. However, its wide flammability range and high burning velocity present a potentially significant hazard. A significant fraction of hydrogen is stored and transported as a cryogenic liquid. Therefore, loss of hydrogen containments may lead to the formation of a pool on the ground. In general, very large spills will give a pool, whereas moderate sized spills may evaporate immediately. Accurate hazard assessments of storage systems require a proper prediction of the liquid hydrogen pool evaporation and spreading.

A new pool model handling the spread and the evaporation of liquid spills on different surfaces has recently been developed in the 3D Computational Fluid Dynamics (CFD) tool FLACS [1-4]. As the influence of geometry on the liquid spread is taken into account in the new pool model, realistic industrial scenarios can be investigated. The model has been validated for LNG spills on water with the Burro and Coyote experiments [5,6]. The model has previously been tested for LH$_2$ release in the framework of the EU-sponsored Network of Excellence HySafe where experiments carried out by BAM were modelled. In the large scale BAM experiments [7], 280 kg of liquid hydrogen was spilled in 6 tests adjacent to buildings. In these tests, the pool spreading, the evaporation, and the cloud formation were investigated. Simulations of these tests are found to compare reasonably well with the experimental results.

In the present work, the model is extended and the liquid hydrogen spill experiments carried out by NASA are simulated with the new pool model. The large scale NASA experiments [8,9] consisted of 7 releases of liquefied hydrogen at White Sand, New Mexico. The release test 6 is used. During these experiments, cloud concentrations were measured at several distances downwind of the spill point. With the new pool model feature, the FLACS tool is shown to be an efficient and accurate tool for the investigation of complex and realistic accidental release scenarios of cryogenic liquids.

1.0 INTRODUCTION AND MOTIVATION

Hydrogen is widely recognized as an attractive energy carrier due to its low-level air pollution and its high mass-related energy density. However, its wide flammability range and high burning velocity present a potentially significant hazard. A significant fraction of hydrogen is stored and transported as a cryogenic liquid (liquid hydrogen, or LH$_2$) as it requires much less volume compared to gaseous hydrogen. In order to exist as a liquid, H$_2$ must be cooled to a very low temperature, 20.28 K. LH$_2$ is a common liquid fuel for rocket applications. It can also be used as the fuel storage in an internal combustion engine or fuel cell for transport applications.

Even though liquid hydrogen tanks can store more fuel in a given volume than compressed hydrogen tanks, there are several downsides to using liquid hydrogen to power large vehicles. One of the most important concerns is that unintended releases (loss of containment) of cryogenic liquids such as LH$_2$

---

[*] Email: prankul@gexcon.com

from storage tanks may spread on the ground (pool formation), evaporate and form a potentially dense hazardous gas cloud. Accurate hazard assessments of storage systems require a proper prediction of the liquid hydrogen pool evaporation and spreading. The size, shape and density of the gas cloud depend on the spill size, shape and evaporation rate. Very few spills of limited size will create a pool, as the liquid hydrogen will evaporate immediately as it comes into contact with the surface. In the cases where a pool is formed, it is necessary to properly model the spill motion and evaporation rate to get a good description of the gas cloud. For liquids spill with boiling point temperature below ambient temperature, most of the heat is transferred from the ground. A good description of the ground is therefore important and it is necessary to handle different surfaces. Another issue that requires attention is the flow above the spill. The source of the spill, terrain, vegetation and buildings will influence the flow field, which only in a few exceptional cases can be considered uniform. This emphasizes the need for a Computational Fluid Dynamics (CFD) tool to calculate dispersion of the gas cloud and, furthermore, a local formulation of the mass and heat transfer between the liquid spill and the surrounding flow.

A model handling releases of liquids on solid ground and sea has been implemented in CFD tool FLACS [1-4]. The shallow water equations are solved with the finite volume method in two spatial dimensions and in time. Sloping terrain and varying ground properties are taken into account. The evaporation rate is calculated locally in each control volume by using expressions from the boundary layer theory, which includes the local turbulence, temperature, and partial pressure of the evaporating specie. The models have primarily been developed to handle LNG releases and have been validated for LNG spills on water with the Burro and Coyote experiments [5,6]. Tests carried out by Exxon have also been used to validate the evaporation rate of LNG on water [3]. These models are applied to LH_2 release experiments to test their applicability.

This paper is organized as follows: The pool model for LNG is presented in Section 2. In Section 3, initial work for modeling LH_2 releases carried out previously is presented [7,10]. Section 4 describes the experiments considered in the present work [8,9]. The results and discussion are presented in Section 5 and the conclusions in Section 6.

2.0 MODEL DETAILS

The CFD-tool FLACS used in this article has been developed since 1980 to model hydrocarbon gas dispersion and explosions in process facilities. During the past three decades extensive validation against experiments has been given high priority in the FLACS development. More details on FLACS can be found at GexCon's web pages and FLACS manual [11,12]. In recent years, there has been significant work to improve the simulation capabilities of FLACS for LNG safety issues. This has been done as the use of LNG has become increasingly frequent around the world and its safety issues recognized. A LNG-development and validation project for FLACS was carried out from 2004-06 with support from StatoilHydro, Total, and Petroleum Safety Authority Norway (PSA), and in cooperation with DNV. A model for liquid spills has been developed in FLACS in this framework. Significant work has been carried out after the end of this project (with the support from Norwegian Research Council) where the model has been developed further (details are given below). The models have been validated using 8 tests from Burro [5] and 3 tests from Coyote experiments performed at China Lake, USA [6]. More details of this validation can be found in [3] and [4].

2.1 The spill model

A liquid will spread until it reaches a steady state where the evaporation rate balances the leak rate or obstacles hinder further pool spread. A spill is driven by gravitational forces in form of differences in the spill height and the shape of the ground while friction forces resist the motion. Pools are spills that are hindered to spread by e.g. embankment and dikes around storage tanks. Uniform flow and circular

pool is typical seen for benchmark tests [1]. In real life, terrain, buildings, process equipment and the source of the spill itself, will disturb the flow field above the pool or spill. Expressions based on boundary layer theory are therefore used to calculate the convective heat and mass transfer in each grid cell separately. Spreading of a liquid spill can be described mathematically by the shallow water equations [13]. Several authors [14,15] have showed that the shallow water equations could describe LNG spills on annular grids. In this work, these are implemented in FLACS. The equation solved for the spill height is given by:

$$\frac{\partial h}{\partial t} + \frac{\partial h u_i}{\partial x_i} = \frac{\dot{m}_L - \dot{m}_V}{\rho_l} \tag{1}$$

The momentum equation is written as:

$$\frac{\partial u_i}{\partial t} + u_j \frac{\partial u_i}{\partial x_j} = F_{g,i} + F_{\tau,i}, \tag{2}$$

where the gravity term is modelled as follows:

$$F_{g,i} = g\Delta \frac{\partial (h+z)}{\partial x_i}, \tag{3}$$

Here, the elevation of the ground has also been included. The parameter Δ equals one for solid surfaces and $\Delta = (1 - \rho_l / \rho_w)$ for spills on water. The shear stress between the spill and substrate is given by the general formula:

$$F_{\tau,i} = \frac{1}{8} f_f u_i |\vec{u}| \tag{4}$$

The transport equation for the specific enthalpy is given by:

$$\frac{\partial \theta}{\partial t} + u_i \frac{\partial \theta}{\partial x_i} = \frac{\dot{m}_L}{h} (\theta_L - \theta) + \dot{q}_c + \dot{q}_{rad} + \dot{q}_g + \dot{q}_{evap} \tag{5}$$

The first term on the right hand side is due to the leak, $\dot{q}_c$ is convective heat transfer, $\dot{q}_{rad}$ is heat transfer to the pool from radiation, $\dot{q}_g$ is heat transfer to the pool from the substrate, and $\dot{q}_{evap}$ is heat loss due to evaporation. Heat transfer from the solid and rough grounds (soil and concrete) is approximated by:

$$\dot{q}_{q,solid} = \begin{cases} \dfrac{\lambda_G (T_G^0 - T_l)(1.5 - 0.25(t - t_{GW}))}{\sqrt{\pi \alpha_G}} & \text{if } t < 4 \text{ sec.} \\[4mm] \dfrac{\lambda_G (T_G^0 - T_l)}{\sqrt{\pi \alpha_G (t - t_{GW})}} & \text{if } t \geq 4 \text{ sec.} \end{cases} \tag{6}$$

In Equation (6), λ_G is the thermal conductivity of the ground, α_G is the thermal diffusivity of the ground and t_{GW} is the time at which the ground is wetted. Infinite ground is assumed in the derivation of the expressions for the heat transferred from the ground in Equation (6).

The governing equations for the spill are discretized on a non-uniform Cartesian staggered grid in two dimensions with a finite volume method. A first-order upwind scheme is employed for the convective

terms in the momentum equation, while a central difference scheme is used for the enthalpy equation. The equations are solved explicitly in time with a 3rd order Runge-Kutta solver.

2.2 Wind modelling

FLACS solves the Reynolds Averaged Navier-Stokes equations by using the k-ε model with the standard set of constants taken from Launder & Spalding [16] for the turbulent closure. Buoyancy effects are taken into account in the turbulent equations. The atmospheric boundary layer is modelled by forcing profiles for the velocity, temperature and the turbulence parameters on inlet boundaries. Wind inlet profiles depend on the Monin-Obukhov length L and the atmospheric roughness length z_0.

The Monin-Obukhov length can be estimated from measurements and it is positive for stable atmospheric boundary layers, negative for unstable boundary layers and infinity for neutral boundary layers. In risk assessment studies, the Monin-Obukhov length is generally not known and must be guessed. An approach is to specify a Pasquill class to determine the Monin-Obukhov length [17]. The inlet profile is logarithmic and can be written as:

$$U(z) = \frac{u_*}{\kappa}\left(\ln\left(\frac{z + z_0}{z_0} \right) - \psi_m \right)$$

(7)

Here, the friction velocity u_* is given by:

$$u_* = \frac{U_0 \kappa}{\ln\left(\dfrac{z_{ref}}{z_0} \right) - \psi_m}$$

(8)

where U_0 is the velocity at the reference height z_{ref}. The constant ψ_m is given by [17,18]:

$$\psi_m = \begin{cases} 2\ln\left(\dfrac{1 + \xi}{2} \right) + \ln\left(\dfrac{1 + \xi^2}{2} \right) - 2\arctan\left(\xi \right) + \dfrac{\pi}{2} & \text{for } L < 0 \\[3mm] -17\left(1 - \exp\left(-0.29\dfrac{z}{L} \right) \right) & \text{for } L > 0 \end{cases}$$

(9)

where $\xi = \left(1 - 16 z/L \right)^{1/4}$.

Equations (7), (8) and (9) complete the specification of the inlet profile. The temperature profile is given as follows:

$$T(z) = T_g + \frac{T_*}{\kappa}\left(\ln\left(\frac{z + z_0}{z_0} \right) - \psi_H \right) - \Gamma_d z$$

(10)

where $\Gamma_d = 0.011 \text{ km}^{-1}$ is the dry adiabatic lapse rate and ψ_H is given as follows:

$$\psi_H = \begin{cases} 2\ln\left(\dfrac{1 + \xi^2}{2} \right) & \text{for } L < 0 \\[3mm] -5\dfrac{z}{L} & \text{for } L > 0 \end{cases}$$

(11)

Turbulence profiles at the inlet are based on the formulation given in Han *et al.* [19] and depend on the atmospheric stability. Expressions for turbulent profiles are not given here for brevity and the interested reader can find them in [4] or [19].

3.0 PREVIOUS WORK INVOLVING LH$_2$ MODELLING

This section describes previous simulations of a liquid H$_2$ release and dispersion experiments. The simulations were performed in connection with a benchmark under the EU-sponsored Network of Excellence (NoE) HySafe. These simulations were a first investigation of the applicability of the pool model developed for LNG pool spread and evaporation to problems involving releases of liquid hydrogen. The model was still under development when these simulations were carried out.

3.1 Experiment, geometry and scenario setup

The simulated experiments were performed by Batelle Ingenieurtechnik and Bundesanstalt fur Materialforschung und Prufung (BAM), Berlin, in the frame of the Euro-Quebec-Hydro-Hydrogen-Pilot-Project and dealt mainly with LH$_2$ near ground releases between buildings. The experiments are described by Statharas, et al. [7], and the description in that paper has been used for definition of the scenarios for the FLACS simulations. The experimental trial 5 was used for simulation due to the fact that in this release the largest numbers of sensor readings were obtained. The experimentalists also carried out their own simulations and compared them to experimental data.

The release occurred between two buildings of length equal to 49.5 m and width 13.4 m. The distance between the two buildings was 23.9 m. The release occurred in the near vicinity of one of the buildings. The release source involved a pipe that was connected to a tank which released the liquid hydrogen into a pan of diameter 0.4 m and height 0.1 m. LH$_2$ was further spilled from this vessel onto a 2 m diameter aluminum plate. Statharas et al. reported an estimated release rate of LH$_2$ of 0.37 kg/s that lasted for 125 s. Based on the estimated release rate it took less than 3 s to fill up the vessel and the total mass of LH$_2$ can be determined as $M_{vessel} = \frac{\pi}{4} \rho_{LH2} D^2 h = 0.89 \, kg$.

Several measurement sensors were used in the experiments. The positions of the sensors which measured H$_2$ concentrations are schematically shown in Figure 1.
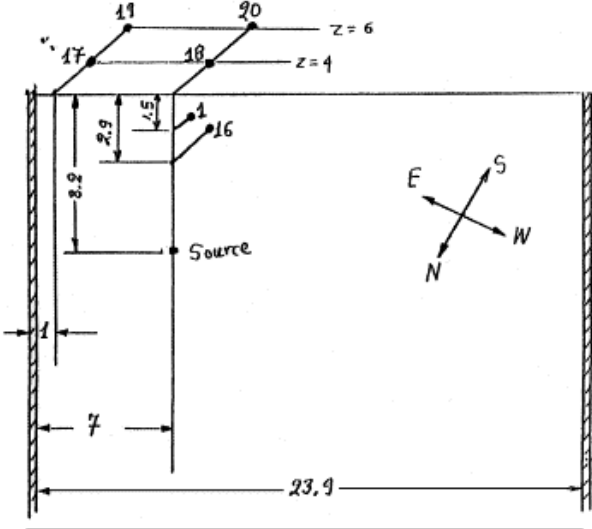
Figure 1 - Sensor and source locations for the BAM experiments (taken from [7])

In the spill region, the size of the grid cells was 40 cm in each direction. The cell size was extended in all directions away from the leak area. The total number of grid cells was 77 000. A neutral stability class was used in the simulations and the estimated average wind speed was 0.5 m/s at a height of 0.9 m. The wind direction was set to be 15° from north. The wind profile given by Equation (7) was set at the inlet boundaries and the profiles of turbulent kinetic energy and turbulent dissipation rate were deduced from the stability class. A no-slip condition was specified at the ground and a passive outflow condition was used at the exits.

3.2 Simulation results

The simulation results are briefly shown below in Figure 2. More details can be found in [10]. The simulated results compare reasonably well with experimental data. The duration where the H_2 concentration is larger than zero is similar to the experiments. The time series of gas concentration at monitors 1, 18 and 20 are acceptable and agree better with experiments than those obtained in the simulations reported in [7]. At monitors 16, 17 and 19 the simulated values are somewhat too high. These three points are located close to the boundary of the extent of hydrogen cloud. These concentrations are therefore very sensitive to local wind speed and direction. A more representative simulation of this local wind field is therefore needed to predict concentrations better.

4.0 NASA RELEASE EXPERIMENTS

The previous section revealed that the spill model could be used to model LH_2 releases with some precision. Encouraged by this, we have applied the current spill model in FLACS to the NASA release experiments. These experiments involving large-scale releases of liquefied hydrogen were carried out at White Sands, New Mexico in the early part of 1980s. The experiments aimed to investigate the generation and dispersion of flammable clouds that could be formed as a result of large, rapid spills of liquid hydrogen. The experiments are described briefly in the present section. More details can be found in [8] and [9].

The experiments consisted of spills of up to 5.7 m^3 of liquid hydrogen ($\approx$ 402 kg), with spill durations of approximately 35 seconds. Instrumented towers located downwind of the spill site gathered data on the temperature, hydrogen concentration and turbulence levels. The spill line used in the experiments dumped the LH_2 into a 9.1 m diameter spill pond, which was constructed of clay sides approximately 60 cm high with compacted sand as a bottom. A 1.2 × 1.2 m steel plate with a thickness of 1.27 cm was located directly under the line exit to prevent earth erosion. Nine 19.5 m towers were deployed downwind of the spill pond, with three towers on a 9.1 m radius 45° apart, three on a 18.3 m radius 45° apart and three towers on a straight line 33.8 m from the centre of spill pond and 22.5° apart with respect to the spill pond, as shown in Figure 3.

Witcofski and Chirivella [8] reported that 7 tests were performed and presented results for test 6. Chirivella and Witcofski [20], presented further details on test 6 and reported that 5.11 m^3 LH_2 was released in 38 s, corresponding to 9.5 kg s^{-1}, (LH_2 density = 70.8 kg m^{-3}). Meteorological conditions for test 6 were 2.2 m s^{-1} wind speed at 10m height, 15 ºC ambient temperature and 29 % relative humidity. Test 6 is used for the present work. Measurements at towers 2, 5, and 7 were reported. These experiments have previously been modelled by Verfondern & Dienhart [21] and Venetsanos & Bartzis [22].
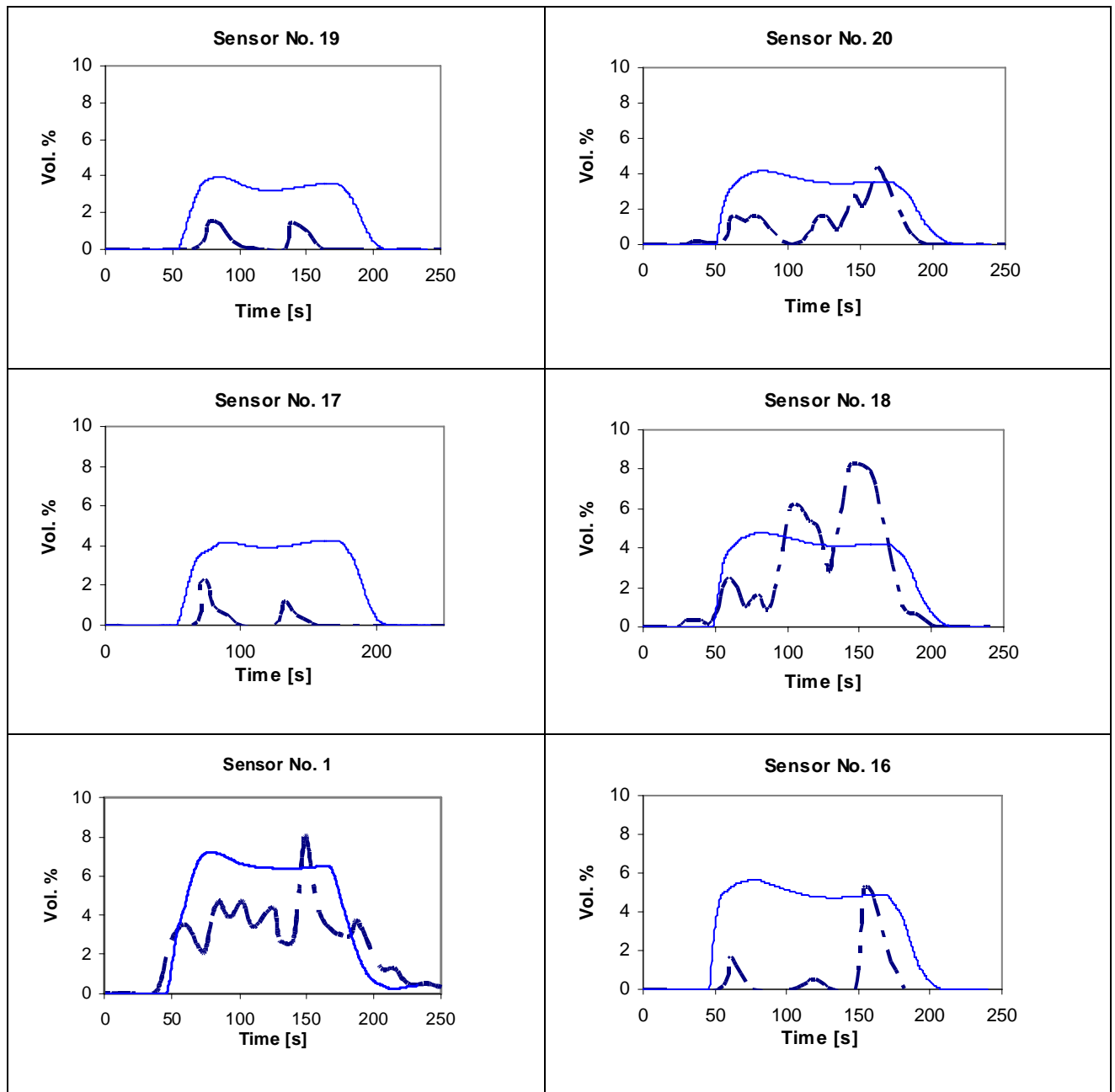
Figure 2 - Comparison of experiments (dotted lines) and simulations (solid lines) for the BAM experiments [7,10]. Top: Sensors 19 and 20, Middle: Sensors 17 and 18, Bottom: Sensors 1 and 16.
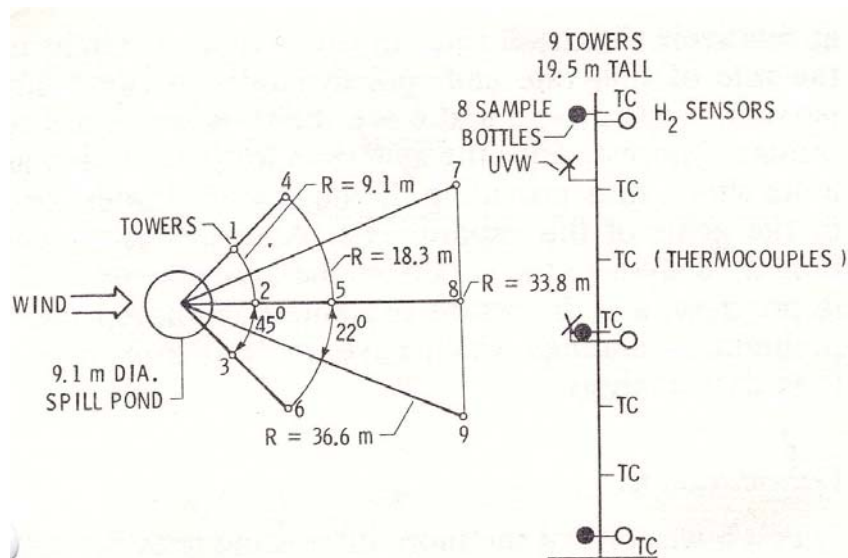
Figure 3 - Deployment of instrumentation towers and typical instrumentation array (taken from [8,9]).

5.0 RESULTS AND DISCUSSION

5.1 Simulation Details

The simulations were performed in a 3D-computational domain with dimensions 130 m × 60 m × 40 m in the X, Y and Z directions. The simulation domain was resolved with a total of 500 000 grid cells. The smallest grid cell had a size of 0.5 m in the horizontal plane and a size of 0.12 m in the vertical plane. The 0.5 m grid cell size in the horizontal plane was kept across the whole spill pond. Liquid hydrogen was released at a rate of 9.5 kg/s into a 9.1 m diameter spill pond. The fence around the spill pond, appreciatively 0.6 m height, was modelled. The steel plate located directly under the line exit to prevent earth erosion was not incorporated into the simulations.

The wind, turbulent kinetic energy and turbulent dissipation rate were set at the inflow boundary. A passive outflow condition at ambient pressure was used at the exit boundary. A no-slip condition at the ground was specified. The wind direction was set aligned with the positive X-direction. The wind speed was 2.2 m/s at 10 m above the ground and the roughness length was 3 mm. The ambient temperature was 15 °C. The spill point had coordinates (0, 0, 0). The inlet boundary was set 15 m upwind of the spill point. The spill was set to start after 10 s of simulation when the wind field was quasi-established in and around the spill pond.

The turbulent and wind profiles at the inlet were deduced from the specification of a Pasquill stability class. Witcofski and Chirivella did not report any information concerning atmospheric stability. Therefore, a sensitivity study was performed with respect to this parameter. Three different Pasquill stability classes were used, namely the very stable (F), neutral (D) and unstable (B) Pasquill stability classes. The effects of low-frequency meandering flow in the atmospheric boundary layer are taken into account by imposing two harmonic waves. More details of this method can be found in [23]. Heat transfer from the ground is a key parameter for both atmospheric stability and plume dispersion. A positive heat flux from the ground (i.e. directed upward) corresponds to an unstable atmospheric boundary layer whereas a negative heat flux corresponds to a stable atmospheric boundary layer. A zero heat flux is associated with a neutral atmospheric stratification. The plume buoyancy is directly related to the temperature of the hydrogen gas cloud. The heat transferred from the ground to the cold plume is thus essential for a proper prediction of the buoyancy and its effect on plume dispersion.

5.2 Results

The predictions for the pool radius and the evaporation rate for the NASA test 6, obtained with FLACS are presented in Figure 4. These parameters are also compared with the results of Verfondern & Dienhart [21], who used the LAuV model. The LAuV model, as the pool model in FLACS, solves the shallow water equation and evaluates the vaporization rate of the liquid. During NASA test 6, some sparse data on the extent of the pool spreading have also been obtained. The observations reported a maximum pool radius ranging between 2–3 m. The predictions of both models over-estimate the pool radius relative to the experimental data. However, FLACS gives the closest prediction. Verfondern & Dienhart [21] explained the over-estimation by the fact that some of the liquid penetrated the sand leading to an increase in the observed vaporization rate and thereby reducing the amount of liquid spreading. In order to account for this phenomenon the thermal conductivity of moist sand which is larger than the one of dry sand has been used in the present simulations. The vaporization rate obtained with FLACS is larger than the one obtained with the LAuV model which is coherent with the observations for the pool radius. The LAuV model neglected all heat fluxes but the heat flux from the ground. Even if the heat flux from the ground is the dominant heat source for pool evaporation, the convective and radiative heat fluxes certainly enhance the vaporization rate. In the experiment, the time elapsed until complete evaporation was estimated to be 43 s which is in very good agreement with the predictions of both models.
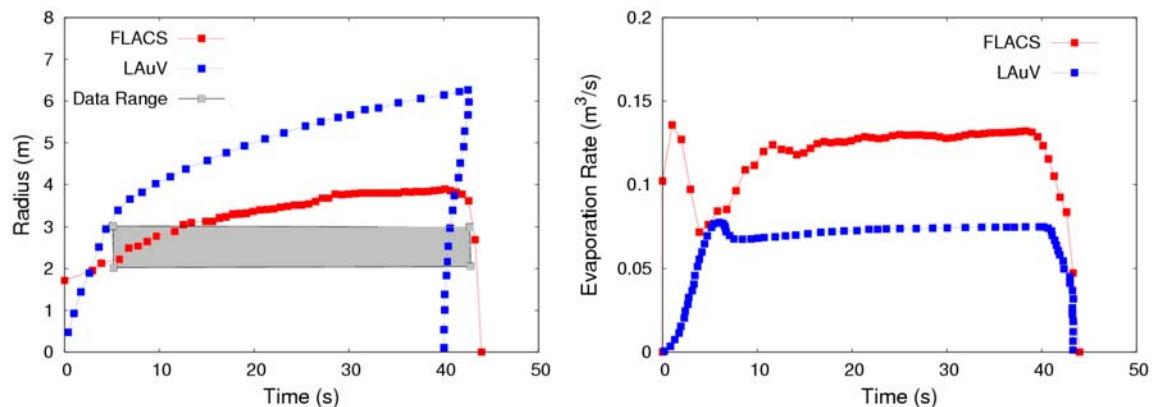
Figure 4 – Comparison of pool spreading and vaporization rate between the FLACS code, the LAuV code and experimental data for NASA Test 6.

Figure 5 presents the predicted gas concentration contours of hydrogen on a volume basis 20 s after the start of the spill for the three stability classes at the position y = 0 m. The Monin-Obukhov length was -9.0 m for the unstable scenario and 8.2 m for the stable scenario. It can be noticed that the use of the different stability classes leads to very different plume behaviours. For the unstable case, the hydrogen is well mixed with the surrounding air due to the very efficient turbulent mixing process in the atmosphere. Increasing the stability from Pasquill class (B) to (F) dampens the atmospheric turbulence and decreases the mixing between hydrogen and the surrounding air. The detachment of the cloud from the ground is only noted for the stable atmospheric class. For the unstable and neutral scenarios the cloud does not detach from the ground in contrast to experimental observations [8,9,20]. It has been observed in the experiments that the plume detached from the ground at about 20 m away from the spill point 20.93 s after the start of the release. This observation compares well with the hydrogen contours of the stable scenario. The experimental results also report that the plume extended to an altitude of about 20 m above ground. In the stable scenario the plume extents 15 m vertically which is reasonably consistent with the experimental observation. The downwind extent of the plume (35–40 m) is also in relatively good agreement with the experimental observation.

Figure 6 shows the simulated hydrogen concentrations as a function of time compared with the experimental data at the different sensor locations. A very good agreement between observed and predicted maximum peaks of hydrogen concentration with the stable configuration is seen for the tower 2 (height 1 m) and for tower 5 (heights 1 m and 9.4 m). For tower 7 (height 9.4 m), a strong under-estimation is noted. It must be mentioned that tower 7 is not located on the axis of the wind but 14 m aside. Wind meandering could be the parameter responsible for the observed peak at this location (see for example [23]). Wind meandering has been implemented in the simulations but does not help in getting a good agreement with experimental data for tower 7. A more advanced investigation of the properties of meandering wind fields would be needed in order to improve the result. It can be observed that with the unstable and neutral atmospheric stratification configurations the hydrogen concentration is over-estimated at the height of 1 m for towers 2 and 5 but under-estimated at the height of 9.4 m for tower 5. This is due to the fact that the hydrogen cloud does not detach from the ground by contrast with the stable configuration.
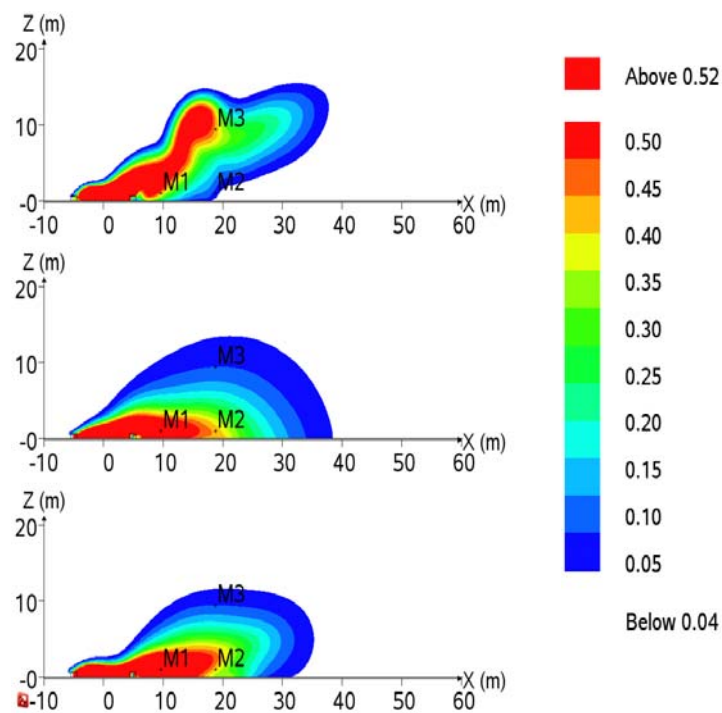
Figure 5 – Volume fraction contours of hydrogen 20s after spill started in the XZ plane at Y = 0 m. [Top] Stable (F) stability. [Middle] Unstable (B) stability. [Bottom] Neutral (D) stability. The annotations M1, M2 & M3 show the positions of the measurement sensors

An additional comment concerns the temperature of the hydrogen vapor in the near proximity of the pool. In the simulation, 10 s after the start of the spill, it was observed that the temperature up to 1 m above the pool is constant and equal to the normal boiling point of hydrogen. From 1 m above the pool, the temperature gradually increases to reach the ambient temperature. At around 3.5 m above the pool, the temperature is 90 K which is the normal boiling point of oxygen. This means that the oxygen and nitrogen (normal boiling point of nitrogen is 77 K) entrained into the hydrogen cloud would condense or even freeze close to the pool (in the first couple of meters above the ground). The hydrogen cloud would be surrounded by a mixture of air-snow and air-droplets which would evaporate and melt as the cloud travels downstream. The presence of the dispersed phase would enhance the dense effects of the hydrogen cloud. This can lead to more severe consequences, especially in hot and dry conditions. This is due to the fact that the condensation of oxygen will start before the condensation of nitrogen (BP 90 K versus 77 K), which means that there may be oxygen lean air, generated but also lots of liquid condensed oxygen which may in a later phase evaporate and generate

oxygen rich air. These effects are not modelled in the present simulations. No quantifications of these condensation and freezing effects were available from the experiments discussed in the present work.
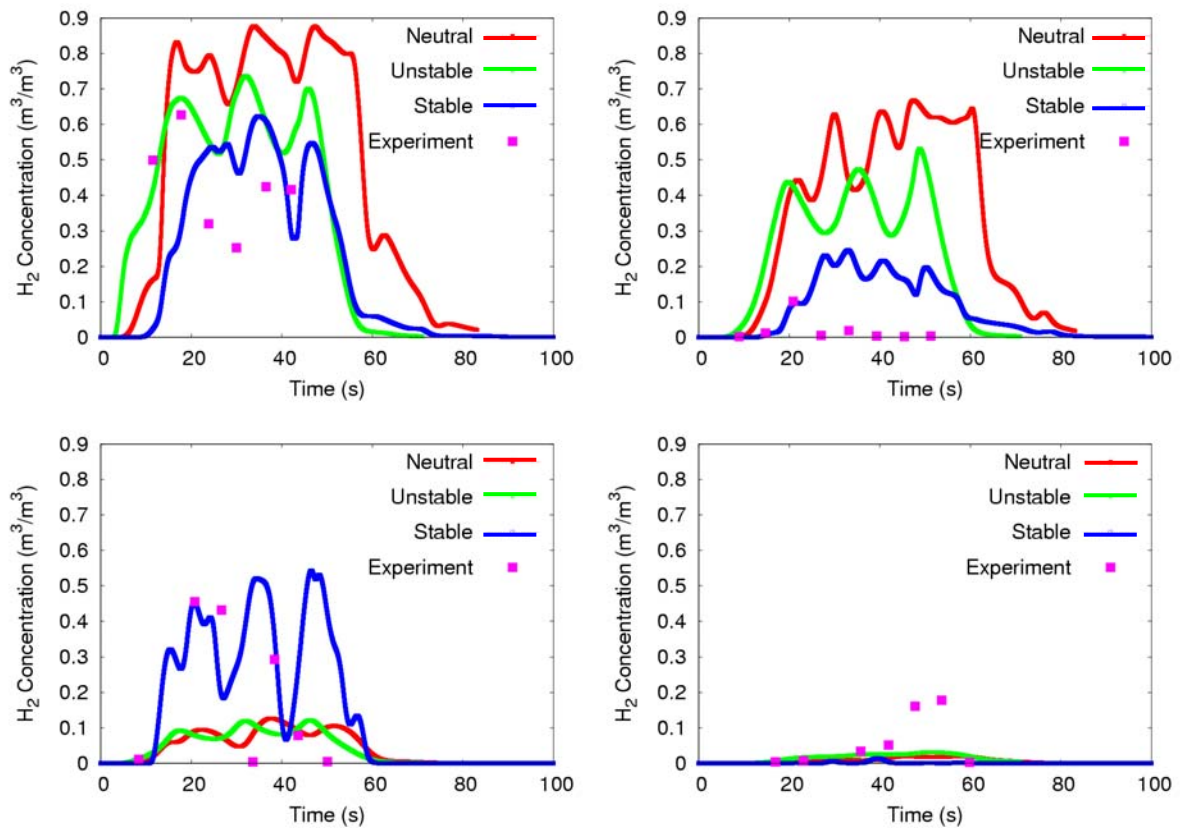
Figure 6 – Time series of hydrogen volume fraction at four different sensors. [Top Left] Tower 2 (height 1 m). [Top Right] Tower 5 (height 1 m). [Bottom Left] Tower 5 (height 9.4 m). [Bottom Right] Tower 7 (height 9.4 m).

6. CONCLUSIONS

The newly developed pool model in the CFD tool FLACS has been applied to handle the spread and the evaporation of the liquid hydrogen spills. Atmospheric stability has been modelled and a sensitivity study on its influence on the dispersion of the hydrogen plume has been performed.

The initial simulations of the BAM experiments showed that FLACS and the new pool model are able to give accurate predictions for the dispersion of hydrogen gas clouds resulting from liquid hydrogen spills in complex environments. The simulated maximum concentrations were within a factor of two for each of the BAM sensors.

Subsequently, simulations of the NASA test 6 consisting of a liquid hydrogen spill and subsequent dispersion of the gas cloud on a flat terrain have been carried out. No information about the atmospheric stability classes was available. A sensitivity study has therefore been performed by using the stable, neutral and unstable stability classes. Gas concentrations contours 25 s after spill started as well as time series of gas concentrations showed that the atmospheric stratification was a key parameter in the dispersion of the hydrogen plume. The stable configuration gave the most coherent results when compared to experimental observations.

7. REFERENCES

1. Hansen, O.R., Melheim, J.A., Storvik, I.E., (2007). CFD-Modeling of LNG Dispersion Experiments. In: AIChE Spring National Meeting, 7th Topical Conference on Natural Gas Utilization, Houston, USA.
2. Hansen, O.R., Melheim, J.A., Storvik, I.E., (2008). Validating the data, LNG Industry Magazine, Spring 2008.
3. Ichard, M., (2008). FLACS-Pool Model Validation: Simulations of the Burro and Coyote test series, GexCon Report 2008-F46212-RA-1 (Confidential).
4. Melheim, J.A., Ichard, M., Pontiggia, M., (2009). Towards a computational fluid dynamics methodology for studies of large scale LNG releases. To be presented in Hazards XXI, 10-12 November, Manchester, UK.
5. Koopman, R.P, Cederwall, R.T., Ermak, D.L., Goldwire jr., H.C., Hogan, W.J., McClure, J.W., McRae, T.G., Morgan, D.L., Rodean, H.C., Shinn, J.H., (1982). Analysis of Burro Series 40-m^3 LNG Spill Experiments, *J. Haz. Mat.*, **6**, 43-83.
6. Goldwire, H.C., et al., (1983). Coyote Series Data Report, Lawrence Livermore Laboratory, UCID 19953.
7. Statharas, J.C., Venetsanos, A.G., Bartzis, J.G., Würtz, J., Schmidtchen, U., (2000). Analysis of data from spilling experiments performed with liquid hydrogen, *J. Haz. Mat.*, **7**, 57-75.
8. Witcofski, R.D., (1981). Dispersion of flammable clouds resulting from large spills of liquid hydrogen, NASA Technical Memorandum 83131.
9. Witcofski, R. D., Chirivella, J. E., (1984). Experimental and analytical analyses of the mechanisms governing the dispersion of flammable clouds formed by liquid hydrogen spills, *Int. J. Hydrogen Energy*, **9** (5), 425-435.
10. Arntzen, B. J., Middha, P., (2008). Modelling of liquid H_2 release and dispersion, GexCon Report 2008-F46207-TN-6.
11. http://www.gexcon.com/index.php?src=flacs/overview.html, Accessed 24th February, 2009.
12. FLACS v9.0 Manual, GexCon R&D, 2009.
13. Toro, E.F., (2001). *Shock-capturing methods for free-surface shallow water flows*. Wiley, UK.
14. Brandeis, J., Ermak, D.L., (1983). Numerical simulation of liquefied fuel spills: Instantaneous and continuous LNG spills on an unconfined water surface, *Int. J. Numer. Methods Fluids*, **3**, 346-361.
15. Woodward, J.L., (1990). An integrated model for discharge rate, pool spread, and dispersion from punctured process vessels, *J. Loss Prev. Process Ind.*, **3**, 33-37.
16. Launder, B.E., Spalding, D.B., (1974). The numerical computation of turbulent flows. *Comp. Meth. In App. Mech. And Eng.*, **3**, 269-289.
17. van den Bosch, C.J.H., Weterings, R.A.P.M., (1997). Methods for the calculation of physical effects due to the release of hazardous materials (liquids and gases), CPR14E, TNO Yellow Book, 3rd edition, TNO, The Hague, The Netherlands.
18. van Ulden, A.P., Holtslag, A.A.M., (1985). Estimation of atmospheric boundary layer parameters for diffusion applications. *J. Clim. Appl. Met.*, **24**, 1196-1207.
19. Han, J., Arya, S.P., Shen, S. Lin, Y.L., (2000). An estimation of turbulent kinetic energy and energy dissipation rate based on atmospheric boundary similarity theory, Tech. Rep. CR-2000-210298, NASA, USA.
20. Chirivella, J. E., Witcofski, R. D., (1986). Experimental results from fast 1500-gallon LH2 spills. *Amer. Inst. Chem. Eng. Symp. Series*, **82**, 120-140.
21. Verfondern, K., Dienhart, B., (1997). Experimental and theoretical investigation of liquid hydrogen pool spreading and vaporization, *Int. J. Hydrogen Energy*, **22**, 649-660.
22. Venetsanos, A.G., Bartzis, J.G., (2007). CFD modeling of large-scale LH2 spills in open environment, *Int. J. Hydrogen Energy*, **32**, 2171-2177.
23. Hanna, S.R., Hansen, O.R., Dharmavaram, S., (2004). FLACS air quality CFD model performance evaluation with Kit Fox, MUST, Prairie Grass, and EMU observations. *Atmos. Environ.*, **38**, 4675-4687.